

## ASSESSMENT OF ANTICYCLONIC SUPERCELL ENVIRONMENTS USING CLOSE PROXIMITY SOUNDINGS FROM THE RUC MODEL

Roger Edwards<sup>1</sup>, Richard L. Thompson and Corey M. Mead  
Storm Prediction Center, Norman, OK

### 1. INTRODUCTION

Anticyclonic, left-moving supercells are a concern for forecasters primarily because of their tendency to yield large and damaging hail and/or unusually large amounts of hail (i.e., Edwards and Hodanish 2004). Such storms may be quite persistent and destructive, lasting several hours with hail approaching 5 inches (13 cm) in diameter (Mathews and Turnage 2000). Further, they may rarely become tornadic, predominantly in environments of moderate to strong buoyancy. Two left-moving supercells that had access to surface-based convective available potential energy (SBCAPE) of near  $2000 \text{ m}^2\text{s}^{-2}$  are known to have produced documented tornadoes -- one in California (Monteverdi et al. 2001) and the other in the Texas Panhandle (Dostalek et al. 2004). Also, a tornadic supercell near Houston, TX on 3 Jun 2003 (NCDC 2003), in an environment of roughly  $5000 \text{ J kg}^{-1}$  SBCAPE, was a left-mover, and is included in our data set.

In the northern hemisphere, some supercells move leftward of the mean wind and vertical wind shear and characteristically exhibit an anticyclonic rotation (mesoanticyclone, after Davies-Jones 1986). Typically, such thunderstorms also move to the left of the lower tropospheric (lowest 3 km layer) hodograph. However, as we will illustrate, variations in low level wind profiles often yield left-mover situations where the net 0-3 km or 0-1 km layer storm-relative helicity (hereafter, SRH) is *positive*. Often, anticyclonic supercells evolve from a storm splitting process, which has been richly documented in the literature in the form of numerical simulations (i.e., Klemp and Wilhelmson 1978, Weisman and Klemp 1982), observational studies (i.e., Nielsen-Gammon and Read 1995, Dostalek et al. 2004), or a blend of observations and numerical methods (beginning with Fujita and Grandoso 1968). Some left-movers form discretely and develop

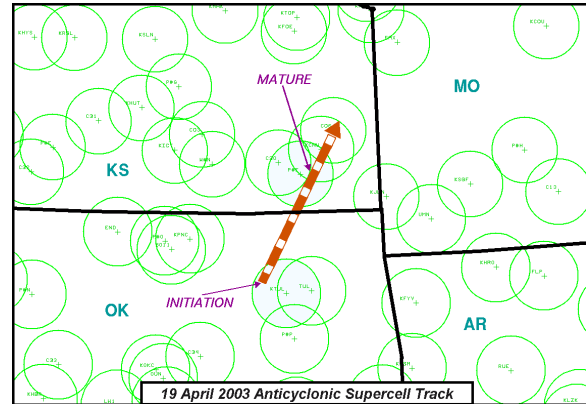


**Figure 1.** Sample left-moving supercell path, with annotations showing location of initiation and mature reflectivity signatures. Range rings are centered on regional RUC point forecast sounding sites with a radius of 40 km; and shaded rings surround the locations of this storm's soundings.

-----

mesoanticyclones *in situ*, foregoing the splitting process.

Climatological studies of anticyclonic supercell environments -- where more than one or two storms comprise the data sample -- are scarce in the literature. One prominent, recent example, however, is Bunkers (2002, hereafter B02), where observed synoptic-scale soundings were gathered for 60 left-moving storms.

### 2. DATA AND METHODS

We examined surface-based, left-moving supercells of both splitting and discrete origins, utilizing 34 Rapid Update Cycle (RUC) proximity soundings from 32 different storms. Thermodynamic data were analyzed using the virtual temperature correction (Doswell and Rasmussen 1994). Severe weather reports for each storm were obtained using either *Storm Data* (NCDC 1999-2003) or the Storm Prediction Center "rough log" of severe weather reports for the most recent supercells for which final *Storm Data* was not yet available.

The viability of RUC soundings for assessing supercellular environments has been validated

---

<sup>1</sup>Corresponding author address: Roger Edwards, Storm Prediction Center, Norman OK.  
E-mail: Roger.Edwards@NOAA.gov

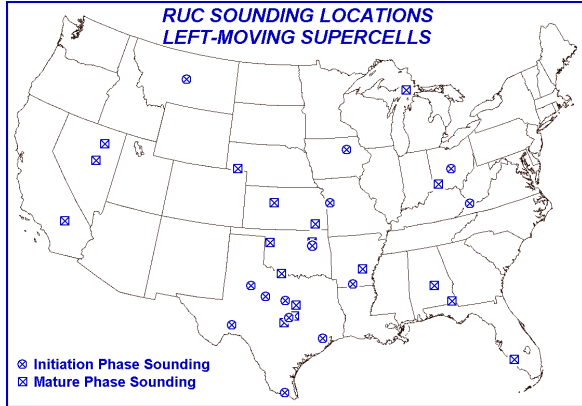


**Figure 2.** Geographic distribution of RUC supercell proximity soundings. Filled squares denote mature phase soundings; filled circles denote initiation phase soundings.

by Thompson et al. (2003, hereafter T03). The storm filtering and sounding analyses in the current study closely resembled the T03 "close proximity sounding" techniques, as applied to mesoanticyclone strength and persistence. Indeed, eight of the soundings in this study, representing eight storms, were culled from the original T03 1999-2001 set, which included both cyclonic and anticyclonic storms (though T03 only published results for the vastly larger cyclonic supercell set). The remainder of our left-moving storm soundings were gathered in 2003 and 2004.

Two crucial refinements were made to the T03 methodology. First we arbitrarily redefined "close proximity" spatially as anywhere within a 40 km radius of a RUC point-forecast sounding site, and temporally at the closest hour to the passage of a storm across the resultant range ring. Therefore, a storm must travel within 40 km and 30 min of an hourly RUC sounding in order to qualify. [By contrast, T03 used RUC grid point soundings bi-linearly interpolated to a surface observation station; whereas the point-forecast soundings are tied to specific surface stations.]

Second, soundings could be taken only from either the initiation point or mature phase of a storm's life span. Two storms (i.e., Fig. 1) passed across enough range rings at fortuitous times to acquire both initiation and mature soundings for the same storm. "Initiation" comprised the first apparent 0.5 deg base reflectivity echo observed in any WSR-88D and directly associated with the sampled storm. If

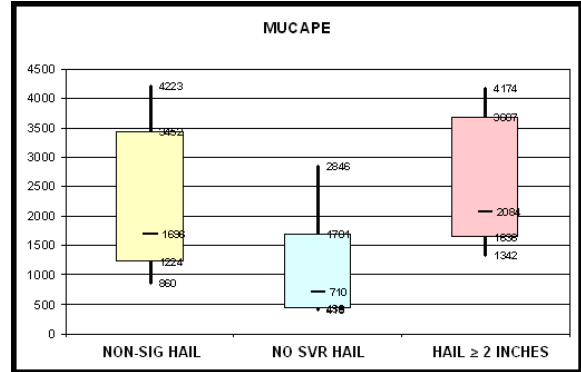


**Figure 3.** Box-and-whiskers diagram representing MUCAPE (y-axis, in  $\text{m}^2\text{s}^{-2}$ ) for left-movers with non-significant hail reports, severe hail reports, and significant hail  $\geq 2$  inches (5 cm). Boxes are bounded by the 75<sup>th</sup> and 25<sup>th</sup> percentiles, and whiskers reach to the 90<sup>th</sup> and 10<sup>th</sup> percentiles.

the left-moving supercell originated from a splitting storm, the initiation point was traced back to the centroid of the first apparent leftward separation from the initially combined echo. "Mature" storms were sampled near peak reflectivity and storm-relative velocity signatures present after  $\sim 2$  hours of lifespan as a discrete composite reflectivity echo; so the minimum lifespan was 2 h. Fig. 1 shows the track of one of the anticyclonic supercells in the data set, and illustrates the size and distribution of close-proximity range rings for sounding sites. The left-moving supercell soundings were widely scattered across the conterminous U.S. (Fig. 2), including storms in the Inter-mountain West and in the subtropics of Texas and Florida.

Severe weather reports, if they existed, were obtained for each of the storms, including hail 0.75 inch ( $\geq 1.9$  cm), measured or estimated gusts  $\geq 50$  kt ( $25 \text{ m s}^{-1}$ ), and/or convective wind damage.

### 3. PRELIMINARY RESULTS

Twenty-three of the 32 storms (72%) yielded severe hail reports. The average and median reports of maximum hail size -- for only those storms producing hail -- were each 4.2 cm in diameter (equivalent to 1.7 inch, or very near the size commonly reported as "golf ball"). This closely approximates the mean and median hail reports for the B02 left-moving supercell set.

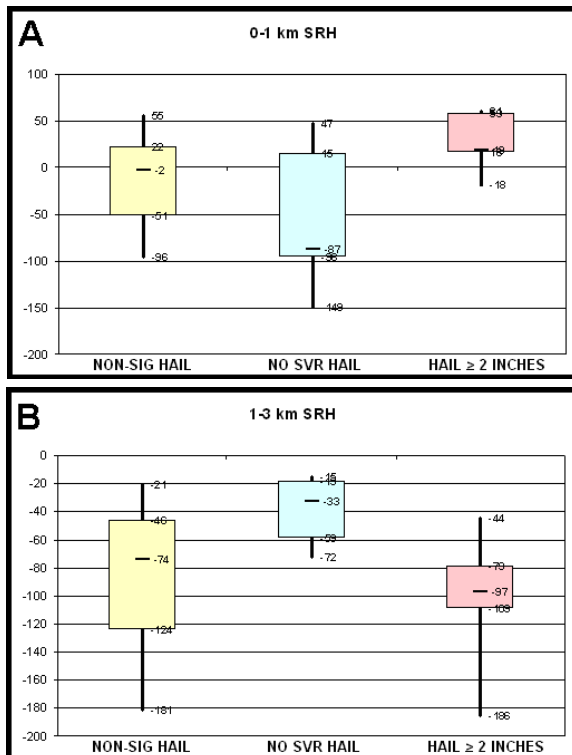


**Figure 4.** Box-and-whiskers diagrams for SRH (y-axis,  $m^2s^{-2}$ ) within the a) 0-1 km layer and b) 1-3 km layer. Storm groupings and percentile bounds for boxes and whiskers are each as in Fig. 3.

Five of the storms (16%) produced significant ( $\geq 2$  inch or 5 cm diameter) hail, the maximum report being 2.5 inch (7.6 cm). While this subset of left movers still is a very small sample, some suggestions are emerging about the relative importance of environmental parameters for significant hail-producing left movers compared to the remainder of storms. One indicator for significant hail was MUCAPE (Fig. 3, where the bottom 25<sup>th</sup> percentile closely approximated the 75<sup>th</sup> percentile for storms with no severe hail reports).

Foremost, perhaps, are great differences in SRH (using the “ID Method” algorithm of Bunkers et al. 2000, hereafter B00) for storms producing significant hail – both by SRH layer used and by comparison with the same SRH layers for storms with no severe hail reported (Fig. 4). Storms producing significant hail tended to occur with *negative* 1-3 km SRH but *positive* 0-1 km SRH. Notably, 1-3 km SRH was negative for all of the storms, as it was for 98% of B02 left-movers. However, 40% of the storms had positive 0-1 km SRH, and 13% had positive 0-3 km SRH.

Eleven (32%) of left-movers produced damaging and/or severe [measured or estimated gusts  $\geq 50$  kt ( $25 m s^{-1}$ )] winds. Little difference was noted in mean MUCAPE ( $135 J kg^{-1}$ , not shown) between those and the storms not producing wind reports. As with significant severe hail, the 1-3 km layer of SRH was the most pronounced in distinguishing severe from nonsevere wind; averaging  $-100 m^2s^{-2}$  for the former and  $-57 m^2s^{-2}$  for the latter.

Observed motions were gathered for each case in the same way as for T03. These in turn were compared to hypothetical storm motions that were derived using the algorithm of B00, which Edwards et al. (2002) independently verified as the most reliable method of approximating supercell motion available at the time. Since it is Galilean-invariant, the B00 left-moving storm technique used here is simply a reversal of sign of the cross-product developed for the right-movers. Finally, a “modified Bunkers” technique was performed (Thompson et al. 2004c), slightly altering the B00 algorithm to incorporate effective lifted parcel levels in the motion estimate. As with unmodified B00 motions, the sign was reversed for left motion.

Motions estimates using B00 and modified B00 were compared to observed storm movements derived as described in T03. The mean absolute errors were  $4.1$  and  $4.3 m s^{-1}$  respectively, in very close agreement with those for left-moving storms in the B02 set. Average B00 errors for  $u$  and  $v$ , respectively, were only  $0.2$  and  $1 m s^{-1}$  respectively. Average modified B00  $u$  and  $v$  errors were also small,  $0.7$  and  $1 m s^{-1}$  respectively, indicating little directional bias with either method. We also computed mean direction errors for B00, which averaged  $-1.4^\circ$  for all storms, with a standard deviation of  $24^\circ$  for the directional errors.

Given the similarities of observed storm motions to those predicted by the negative of the B00 algorithm, we confidently can use the latter (modified or unmodified) in derived diagnostics that rely on storm motion estimates.

From there we devise a Left-moving Supercell Composite Parameter (LSCP) as a complement to existing SCP versions (T03, Thompson et al. 2004a) for right moving storms, in order for forecasters to quickly diagnose environments suitable for the development and maintenance of anticyclonic supercells. The LSCP is identical to

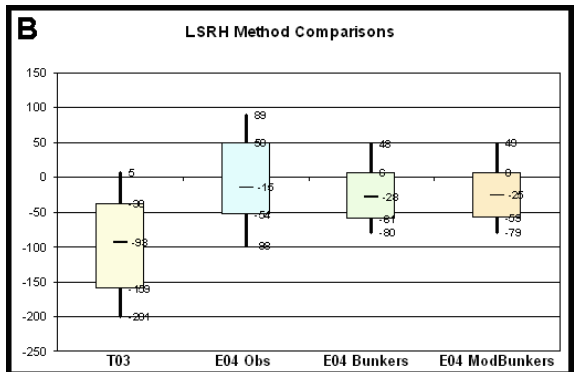
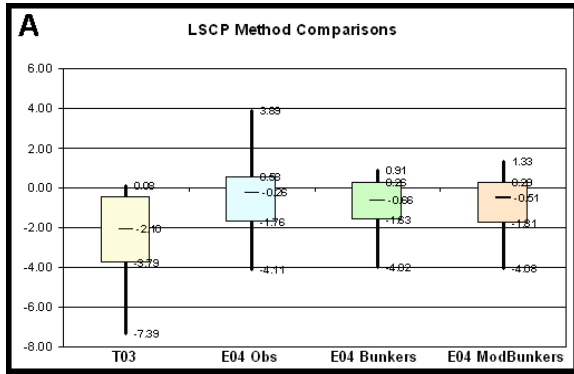


**Figure 5.** Diagrams comparing a) LSCP and b) LSRH, for the left-moving storm set, utilizing surface-based parcels as in the Thompson et al. 2003 (T03) method for SCP, effective parcel with observed storm motions (E04 Obs), effective parcel with ground-based B00 algorithmic motions (E04 Bunkers), and effective parcel with B00 motion adjusted to the effective surface (E04 ModBunkers). Percentile conventions for boxes and whiskers are as in Fig. 3.

the latest formulation of SCP (Thompson et al. 2004b) except for the reversed sign of the propagation vector input to the storm-relative helicity component:

$$\text{LSCP} = (\text{MUCAPE} / 1000 \text{ J kg}^{-1}) * (\text{ELSRH} / 50 \text{ m}^2\text{s}^{-2}) * (\text{ESHR} / 20 \text{ ms}^{-1})$$

MUCAPE is most unstable parcel CAPE and ELSRH is effective SRH (Thompson et al. 2004c), but with the sign of the B00 propagation vector reversed. When effective shear ESHR  $< 10 \text{ ms}^{-1}$ , the term is set to 0 and LSCP=0. For ESHR  $> 20 \text{ ms}^{-1}$ , the term is set to 1. For ESHR of  $10\text{-}20 \text{ ms}^{-1}$ , the values are incorporated directly. Thresholds for nonzero LSCP are MUCAPE  $\geq 100 \text{ J kg}^{-1}$  and convective inhibition  $< 250 \text{ J kg}^{-1}$  (Thompson et al. 2004a).

LSCP computations for the data set were compared across observed motion and both versions of B00, as well as to the negative of the SCP formulation from Fig. 5a. Mean LSCPs (not shown) show similar trends, at -3.5 for the T03 method, -.24 for observed motions and effective parcels, -.75 for effective parcels with B00, and -.7 for effective parcels and modified B00. Note that the effective surface can be slightly above the ground surface even where storms have some SBCAPE (Thompson et al., 2004b and 2004c). Still, the difference in impact of modified and unmodified B00 algorithms was negligible, indicating no change in relative utility for either in judging the potential for surface-based left-movers. This is consistent with the concept of effective parcels being at or near surface for storms with SBCAPE.

The separation in distribution of effective parcel LSCP from T03 computation LSCP can be tied to helicity. All three LSCPs incorporating effective parcels were less negative, in the median, than LSCP using T03 standards. This can be attributed to the effects of LSRH in LSCP (Fig. 5b), which was significantly more negative using T03. ELSRH for surface-based storms sometimes fails to extend well into the 2-3 km layer, truncating much of the negative helicity contribution present in T03 and indicated by Fig. 4b here.

This trend also was evident in comparisons of mean LSRH methods for storms producing significant hail, and separately, for storms producing severe wind (not shown). Using T03, LSCP averaged -6 for storms with severe wind compared with -2.3 for the effective parcel based LSCPs. The absolute differences between severe and nonsevere wind was smaller for the effective LSCP formulations, generally -0.1 less for severe wind producing left movers.

#### 4. CONCLUSIONS AND DISCUSSION

In their investigation of a single left-moving, tornadic supercell in the Texas Panhandle, Dostalek et al. (2004) presumed a simple reversal of sign of SRH, from the negative SRH ranges of the Rasmussen and Blanchard (1998) supercell climatology, as an adequate indicator of environmental suitability for anticyclonic supercells. Their storm's SRH complied with that assumption; however the preliminary results

do not support categorically extending such a conclusion to a multitude of left-moving supercells. With substantial leftward deviations from the mean wind vector by boundary layer flow vectors, thunderstorms sometimes do move leftward of either the vertical shear or mean wind, but rightward of much of the lowest 1-2 km hodograph. This often results in slightly negative total SRH within the lowest 3 km, but a positive value through some substantial subset of that layer near the surface. The assessment more closely resembled that of B02, who found 25% (65%) of 0-3 km (0-1 km) SRH was positive because of the clockwise hodograph curvature in those layers. Also, all the storms carried negative 1-3 km SRH, as did all but one storm in B02. The preliminary results, therefore, strongly support the B02 conclusions about the relative importance of 1-3 km SRH as a left-moving supercell indicator.

The contribution of 1) a pronounced small-sample signal from 0-1 km SRH to ELSRH for significant hail producing storms that are surface-based (therefore making the effective surface at ground level) and 2) substantially larger MUCAPE for most such storms, indicates that LSCP may be useful as an indicator of exceptionally damaging hail.

A check of the Thompson et al. (2004a) database revealed significant hail from right-moving supercells within a few hundred kilometers and 1-2 h of the left-movers on four of the five left-moving significant hail cases, and in the fifth, the reported hail size was 1.75 inch (4.4 cm), just below significant criteria. For the significant hail producing left-movers, the average *right* SCP was 15, while the left movers without severe hail had a mean *right* SCP an order of magnitude less at 1.1. As mentioned above, the left movers with no severe hail also had substantially lower CAPE, more *positive* 0-1 km LSRH, and more *negative* 1-3 km LSRH. These findings indicate that significant hail in left-moving supercells could be nowcast using strongly negative 1-3 km SRH, large *right* SCP, and the presence of a leftward-deviant storm. In such settings more curvature often exists in the 0-1 km hodograph (B02) – trending SRH positively in that layer even for left motion – and nearby right-moving storms also tend to produce destructive hail. Of course the sample of significant hail producing left-movers must grow before these results can be considered more than preliminary.

Similar but less pronounced trends were found with severe wind producing left-movers, not only in LSCP and its component LSRH, but in right SCP (slightly more than double the values for nonsevere wind producers). This suggests a weaker but still potentially useful application of LSCP and SCP to nowcasting severe/damaging wind from left-moving supercells. For both wind and hail, it appears that computing LSCP using the T03 method may be a stronger indicator of severe potential overall, given the findings of greater negative LSCP numbers for both severe wind and significant hail than for LSCP formulae incorporating effective parcels.

Future work will examine elevated anticyclonic storms in extensions of this work after accumulating a larger sample of all classes of cases. One way to do so will be to test the relative utility of the modified version of the B00 motion algorithm that accounts for supercells rooted off the surface using effective parameters.

We also will construct composite hodographs for the expanded data set of left-movers and compare those to the B02 findings. Composite hodographs also will be compared for the subsets of storms producing significant hail and no severe hail, to complement aforementioned comparisons using SRH layers (i.e., Fig. 3).

This database will be expanded with additional cases as they occur, for a more robust sample size of both total storm numbers and significant hail producers, and to introduce a set of elevated storms large enough in numbers to analyze meaningfully. Initiation and mature-phase sounding groups will be analyzed and compared to determine if any systematic environmental changes occurred during the evolution of these storms. No distinct analysis may be done with tornadic left-movers until and unless their sample size increases substantially beyond the lone storm in the set; however the Houston area event may warrant its own case study, perhaps in comparison with the two other documented tornadic left-movers.

Finally, simulations have indicated that the longevity of left-moving supercells may be tied strongly to storm-scale processes occurring well below the resolution of operational models such as the RUC, such as ingestion of relatively cold and stable downdraft air resulting from a combination of their storm-relative inflow and



structural alignment (i.e., Grasso 2000). Such indications -- along with some of the findings herein, and other aspects of storm splitting and mesoanticyclonic environments -- depart from linear theory of left- and right-moving supercell symmetry, persistence and strength. As such, they are potentially critical to the warning process and are strongly recommended for investigation by observational field projects.

## 5. ACKNOWLEDGMENTS

Thanks goes to Steve Weiss for his careful review, and to the Science Support Branch of SPC for supplying data access and storage. We appreciate the programming efforts and assistance provided by John Hart and Gregg Grosshans of SPC, enabling us to more efficiently analyze the data.

## 6. REFERENCES

- Bunkers, M.J., 2002: Vertical wind shear associated with left-moving supercells. *Wea. Forecasting*, **17**, 845-855.
- \_\_\_\_\_, B.A. Klimoski, J.W. Zeitler, R.L. Thompson, and M.L. Weisman, 2000: Predicting supercell motion using a new hodograph technique. *Wea. Forecasting*, **15**, 61-79.
- Davies-Jones, R.P., 1986: Tornado dynamics. *Thunderstorm Morphology and Dynamics*. 2nd Ed., E. Kessler Ed., University of Oklahoma Press, 197-236.
- Dostalek, J.F., J.F. Weaver and G.L. Phillips, 2004: Aspects of a tornadic left-moving thunderstorm on 25 May 1999. *Wea. Forecasting*, in print.
- Doswell, C.A. III, and E.N. Rasmussen, 1994: The effect of neglecting the virtual temperature correction on CAPE calculations. *Wea. Forecasting*, **9**, 625-629.
- Edwards, R., R.L. Thompson, and J.A. Hart, 2002: Verification of supercell motion forecast techniques. Preprints, *21st Conf. on Severe Local Storms*, San Antonio, TX, Amer. Meteor. Soc., J57-J60.
- \_\_\_\_\_, and S.J. Hodanish, 2004: Environmental analysis and photographic documentation of an intense, left-moving supercell on the Colorado plains. Preprints, *22nd Conf. on Severe Local Storms*, Hyannis, MA, Amer. Meteor. Soc. (this volume).
- Fujita, T.T., and H. Grandoso, 1968: Split of a thunderstorm into cyclonic and anticyclonic storms and their motion as determined from numerical model experiments. *J. Atmos. Sci.*, **25**, 416-439.
- Grasso, L.D., 2000: The dissipation of a left-moving cell in a severe thunderstorm environment. *Mon. Wea. Rev.*, **128**, 2797-2815.
- Klemp, J.B., and R.B. Wilhelmson, 1978: Simulations of right and left moving storms produced through storm splitting. *J. Atmos. Sci.*, **35**, 1097-1110.
- Mathews, G.N., and T.J. Turnage, 2000: An example of a left-split supercell producing 5-inch hail: The Big Spring, Texas storm of 10 May 1996. Preprints, *20th Conf. on Severe Local Storms*, Orlando, FL, Amer. Meteor. Soc., 526-529.
- Monteverdi, J.P., W. Blier, G.J. Stumpf, W. P, and K. Anderson, 2001: First WSR-88D documentation of an anticyclonic supercell with anticyclonic tornadoes: The Sunnyvale-Los Altos, California, tornadoes of 4 May 1998. *Mon. Wea. Rev.*, **129**, 2805-2814.
- NCDC, 1999-2003: *Storm Data*. Vols. 41-43 and 45. [Available from National Climatic Data Center, Asheville, NC, 28801.]
- Neilsen-Gammon, J.W., and W.L. Read, 1995: Detection and interpretation of left-moving severe thunderstorms using the WSR-88D: A case study. *Wea. Forecasting*, **10**, 127-140.
- Rasmussen, E.N., and D.O. Blanchard, 1998: A baseline climatology of sounding-derived supercell and tornado parameters. *Wea. Forecasting*, **13**, 1148-1164.
- Thompson, R.L, R. Edwards and C.M. Mead, 2004a: An update to the supercell composite and significant tornado parameters. Preprints, *22nd Conf. on Severe Local Storms*, Hyannis, MA, Amer. Meteor. Soc. (this volume).
- \_\_\_\_\_, C.M Mead, and R. Edwards, 2004b: Effective bulk shear in supercell thunderstorm environments. Preprints, *22nd Conf. on Severe Local Storms*, Hyannis, MA, Amer. Meteor. Soc. (this volume).
- \_\_\_\_\_, Edwards, R., and C.M. Mead, 2004c: Effective storm-relative helicity in supercell thunderstorm environments. Preprints, *22nd Conf. on Severe Local Storms*, Hyannis, MA, Amer. Meteor. Soc. (this volume).

\_\_\_\_\_, R. Edwards, J.A. Hart, K.L. Elmore and P. M. Markowski, 2003: Close proximity soundings within supercell environments obtained from the Rapid Update Cycle. *Wea. Forecasting*, **18**, 1243-1261.

Weisman, M.L., and J.B. Klemp, 1982: The dependence of numerically simulated convective storms on vertical wind shear and buoyancy. *Mon. Wea. Rev.*, **110**, 504-520.